

Numerical Simulation of Ryugu’s Thermophysical Properties using the Discrete Element Method

B. Agrawal¹, M. Grott¹, J. Knollenberg¹, J. Biele², B. Gundlach³, J. Blum⁴

¹German Aerospace Center, Berlin, Germany, ²German Aerospace Center, Köln, Germany, ³Westfälische Wilhelms-Universität Münster, Germany, ⁴Technische Universität Braunschweig, Germany

Between June 2018 and November 2019, the Hayabusa2 mission [1] investigated the near-Earth asteroid (162173) Ryugu. The main objective of the mission was to study this pristine C-type asteroid to better understand the origin and evolution of materials in the early solar system. Hayabusa2 deployed the MASCOT lander in October 2018 and following a detailed remote sensing and in-situ investigation, Hayabusa2 returned samples to Earth in December 2020. A summary of main findings of the mission was recently reviewed by [2], who also compared results obtained during the remote sensing, in-situ, and sample analysis phases.

The detailed study of Ryugu over scales ranging from the micro (sample) scale to global remote sensing data revealed that while several properties derived from remote sensing and in-situ analysis agree very well with results obtained from the sample analysis, some discrepancies exist [2]. These scale dependent effects include properties like reflectance and thermophysical properties. Here, we focus on the derived thermal properties, which were determined using MASCOT’s MARA radiometer [3], the Hayabusa2 orbiter’s TIR thermal infrared imager [4], as well as the returned samples [5]. While in-situ and remote sensing data roughly agree, yielding thermal inertias of $282_{-25}^{+93} \text{ Jm}^{-2}\text{K}^{-1}\text{s}^{-1/2}$ [6, 7] and $225 \pm 45 \text{ Jm}^{-2}\text{K}^{-1}\text{s}^{-1/2}$ [4, 8], respectively, sample analysis indicates values of $890 \pm 45 \text{ Jm}^{-2}\text{K}^{-1}\text{s}^{-1/2}$ [5], which are thus about three times as large.

The reason for the observed scale dependence of the thermophysical properties remains unknown, but it has been proposed that the difference could be caused by a thermal shielding effect on intermediate scales [5]. Cracks may, for example, be generated by thermal fatigue and a conceptual model of how these cracks may be distributed inside boulders is shown in the left panel of Fig. 1. Thermal fatigue would extend to a few skin depths $d_c = \sqrt{\kappa P/\pi}$, where $\kappa = k/\rho c_p$ is thermal diffusivity, ρ is density, c_p is specific heat, and P is the period of the forcing (a day-night cycle). Remote sensing instruments like MARA and TIR are sensitive to material over a similar depth range, while samples could contain considerably less cracks.

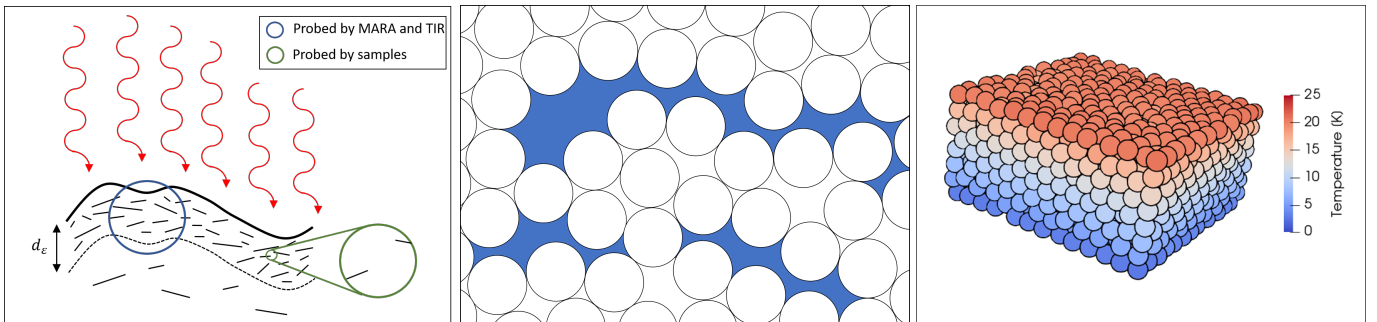


Figure 1: Left: Conceptual model of scale dependence of thermophysical properties. The range of materials sampled by the in-situ and remote sensing instruments MARA and TIR is indicated in blue, while the returned samples are indicated in green. On large scales, the material may exhibit abundant cracks due to insolation induced fatigue, while samples may contain only few cracks. Middle: Modeling approach including cracks induced by thermal fatigue using discrete elements. Fatigue induced cracks separating particles are indicated in blue. Right: First results of simulating heat flow through a bed of monodisperse particles without cracks. Colour represents particle temperatures going from red (hot) to blue (cold).

Our project focuses on exploring this discrepancy and formulating a thermophysical model of the boulders including cracks and sintering. To understand the thermophysical properties of asteroids, we base our model on the LIGGGHTS(R)-PUBLIC package [9]. It is an open source discrete element method particle simulation software built for simulating general granular motion and atomic/molecular dynamics. The program integrates Newton’s equations of motion for a large collection of spherical particles which interact via short or long range forces. The inter-particle forces are determined based on a user selected contact model which can encompass interactions such as elastic (contact) forces, rolling friction, cohesion and surface geometry of particles. In addition to mechanical interactions, the package can also be used to study the thermal energy transport between particles in contact. This is governed by

the thermal conductivities of the particles and their contact areas. Here we specify contact areas as the cross section of the geometrical overlap of two spherical particles. Upon introducing cracks in a random packing of monodisperse particles (middle panel in Fig. 1), we intend to study the thermal properties of the bulk material.

As a benchmark test for the numerical code we calculate the steady-state heat flow through a particle-bed to reproduce the relation between thermal conductivity, contact areas, and particle radii. Once in thermal equilibrium, thermal conductivity of the bed can be calculated given the specified temperature boundary conditions and resulting heat flux through the bed. This can then be compared to analytical and experimental results for monodisperse particles [10]. First results of the simulation are shown in the right hand panel of Fig. 1 where heat is flowing vertically downwards through a bed of cohesion-less particles with adiabatic boundary conditions elsewhere.

Once the numerical method has been benchmarked using monodisperse cohesion-less particles, we will include polydisperse particles and a parameterized description of enhanced heat transport through inter-particle bonds. Using the contact area as a tuning parameter we fit the numerical results to the thermal properties, as derived from sample analysis [5]. Then, cracks will be introduced as outlined in the middle panel of Fig. 1 and the associated reduction in thermal conductivity will be investigated. In this way, we will systematically study the amount of material disruption necessary to match the remote sensing observations [7, 6, 4].

References

- [1] Sei-ichiro Watanabe et al. In: *Space Science Reviews* 208.1 (July 2017), pp. 3–16.
- [2] Katharina Otto et al. In: *Earth, Planets and Space* 75.1 (Apr. 2023), p. 51.
- [3] M. Grott et al. In: *Space Science Reviews* 208.1 (July 2017), pp. 413–431.
- [4] Tatsuaki Okada et al. In: *Nature* 579.7800 (Mar. 2020), pp. 518–522.
- [5] T. Nakamura et al. In: *Science* 379.6634 (2023), eabn8671.
- [6] Maximilian Hamm et al. In: *Planetary and Space Science* 159 (2018), pp. 1–10.
- [7] M. Grott et al. In: *Nature Astronomy* 3.11 (Nov. 2019), pp. 971–976.
- [8] Yuri Shimaki et al. In: *Icarus* 348 (2020), p. 113835.
- [9] Christoph Kloss et al. In: *Progress in Computational Fluid Dynamics* 12.2-3 (2012), pp. 140–152.
- [10] N. Sakatani et al. In: *AIP Advances* 7.1 (Jan. 2017), p. 015310.